Recent progress in experimental studies of electro-hydrodynamic flow in electrostatic precipitators

Recent progress in experimental studies of electro-hydrodynamic flow in electrostatic precipitators

J Mizeraczyk[1,2*], J Podlinski[1], A Niewulis[1] and A Berendt[1]
1 Centre for Plasma and Laser Engineering, The Szewalski Institute of Fluid Flow Machinery, Polish Academy of Sciences, Fiszera 14, 80-952 Gdansk, Poland
2 Department of Marine Electronics, Gdynia Maritime University, Morska 81-87, 81-225 Gdynia, Poland

E-mail: jmiz@imp.gda.pl

Abstract. Many experimental, theoretical and numerical works were devoted to the electrohydrodynamic (EHD) flow generated in electrostatic precipitators (EPSs). The generally accepted conclusion from these studies is that the EHD flow plays an important role in the particle collection in ESPs. However, despite of the recent fast progress in numerical simulation and experimental techniques used in the ESPs studies many problems related to the influence of the EHD flow on the performance of ESPs are unsolved. In particular, the influence of the turbulent EHD on submicron particles transport and deposition in ESPs is ambiguous. This problem and other related to the particle collection in ESPs are objectives of this paper, basing on the recent progress in experimental investigations of the EHD flow in ESPs.

1. Introduction

1.1. EHD effects in gaseous media - The state of the art

Electrohydrodynamics (EHDs) is devoted to the investigation of motion of electrically charged fluids (gaseous or liquid) subjected to an electric field, usually external. In a single-phase fluid the forces exerted by the external electric field on free or polarization charges present in the fluid are transferred during collisions to the neutral molecules, causing a change of their previous motion (called a primary flow). As a result a secondary flow appears. The secondary flow causes a redistribution of the electrical charges, which in turn modifies the electric field in the fluid. Such a coupling of the electric field, the space charge formed by the electrical charges [1-5], and the fluid flow makes the EHDs a difficult subject [6-8]. The difficulty rises when the fluid consists of two or more matter phases (the case of multi-phase fluid). An example of the two-phase fluid is a flow of flue gas, that can be regarded as a mixture of an after-combustion gas and dust (a particulate matter). In this case, the particulate matter become charged by the gaseous ions and get subjected to the electrical field. Due to it the charged particles form its own secondary flow, usually different from that of the molecular secondary flow. In this case the EHD interaction includes the electric field, the molecular space charge, the particle space charge, and the flow of the carrier-fluid. As a result the EHDs of such a multi-phase

* To whom any correspondence should be addressed.

fluid becomes very complex, not only from the phenomenological point of view, but also for theoretical and experimental studies.

EHDs covers also such particle and fluid transport mechanisms as: electrophoresis, electrokinesis, dielectrophoresis, electro-osmosis and electrorotation which occur in gaseous and liquid media.

The subject of this paper is restricted to EHD phenomena in a gaseous medium. Systems with EHD effect in a gaseous medium [9] are used commercially in a wide range of industries. The most important is filtration and separation of dust particles in ESPs, which are by far the most common electrostatic devices used in pollution control.

Another electrostatic system with EHD effect is an electrostatically enhanced cyclone separator [10, 11]. A cyclone separator provides a reasonably effective means of removing dust particles exceeding 5 um in diameter from a gas stream, but its efficiency falls off rapidly as the particle size of the dust decreases. A significant improvement in small-size dust particle removal efficiency has been reported with an electrostatically enhanced cyclone. The particle removal in the electrostatic part of cyclone depends apparently on the flow pattern modified by the EHD forces. However, no in-depth research study are reported on that subject.

EHD effect plays an important role in collection of small pollutant particles in electrostatic scrubbers [12, 13]. In a conventional scrubber, water droplets (collector particles) are sprayed through a polluted gas stream and particles are collected by inertial impaction. The collection efficiency for fine pollutant particles is poor as these tend to follow the gas streamlines round the collector particles, avoiding settling on them. However, the collection of micron and submicron pollutant particles can be significantly improved by charging the pollutant and collector particles to opposite polarities. Some improvement can be still obtained if only the collector particles are charged. Both charging results in the appearance of EHD forces which change the flow conditions inside the scrubber. In particular the EHD forces influence the trajectories of the pollutant particles due to the attraction between them and the collector particles. The improvement of the pollutant particle collection due to the EHD forces concerns mainly the particles of sizes in the range of 0.1 to 1 μm, where the collection efficiency due to inertial impaction is low, but Brownian diffusion does not yet dominate over other collection processes.

Electrostatic atomisation [14-16] is an important example of using EHD forces to disrupt a liquid surface and form a highly charged stream of droplets, which are smaller than those when a liquid is atomised mechanically. EHD atomisation are used in many diverse applications, including paint spraying, spray and powder coating, and electrostatic printing. It has been also proposed as a mechanism for the propulsion of space vehicles.

EHD forces have also been proposed to be used for controlling gaseous (and also liquid) flows in the so called EHD pumps without mobile parts [17-20]. In natural sciences, EHD is indispensable to understand atmospheric electricity.

A newly emerging application of EHD phenomenon is the controlling of air flow [21-24]. For that purpose plasmas of a dielectric-barrier discharge (DBD), corona discharge and spark plasma are employed.

Plasma-based devices for active airflow controlling (called EHD flow actuators) convert electric energy into kinetic energy without involving moving mechanical parts [25-31]. Their response time is very short and they enable a real-time airflow controlling at high frequency [32-39]. Besides, they can reduce the flow-induced noise. EHD flow actuators are very attractive because they do not exhibit many drawbacks typical of mechanical air flow devices. Active air flow control is a hot topic in industrial aeronautics.

Most aspects of EHD phenomenon may be illustrated using an example of electrostatic precipitator [40-42] where the EHD forces are responsible for the collection of dust particles. The majority of EHD effects present in ESPs [43-52] are typical of other gaseous EHD systems. Analyzing the imperfections of the performance of ESPs related directly or indirectly to EHD phenomenon allows us to make a list of the fundamental problems that should be solved to deeply understand this phenomenon, and then implement the attained knowledge in practice.

The ESPs have received the intensive study in their hundred year history. Nowadays they operate with high overall dust particle collection efficiency (99.5 %), however, are not effective in removing the fine particles (below 1 um). This is attributed to poor understanding of the performance of ESPs, operation of which depends on EHD phenomena. Many fine particles of a size of 1 um or less, emitted by ESPs contain toxic trace elements and are dangerous for human beings and animals. Recently, a special environmental concern in the form of tough regulations is directed towards controlling the emission of micron and submicron particles by ESPs. This forces an action towards the improvement of ESPs. However, industrial ways of increasing the fine particle collection are limited, and without studies of the fundamental phenomena occurring in an environment similar to that of ESPs the further progress in this field is doubtful.

A theory for ESPs with turbulent flow was developed by Deutsch in 1922 [53]. In this theory, turbulent mixing is assumed to form a uniform distribution of dust particles, which then have a uniform concentration C throughout a given cross section of the ESP duct. Inside the precipitator the particles experience an electrostatic force which give them a velocity (w) towards the collecting walls. This velocity is called the migration velocity. According to the Deutsch theory the collection efficiency (η) of a precipitator is given by the formula:

$$\eta = (C_{in} - C_{out}) \cdot (C_{in}) = 1 - \exp(-A\, w \cdot (u_g)^{-1}) \quad (1)$$

where C_{in} and C_{out} are the inlet and outlet concentration of dust particles, A is the total collecting area, and u_g is the volume flow rate of the gas. This formula describes the precipitator collection efficiency in terms of known or measurable parameters.

It has long been known that the Deutsch equation overestimates the efficiency of full-scale precipitators [40]. Not surprisingly many modifications of the Deutsch theory have been made. However, because of a large number of approximations made in the derivation of modified Deutsch's equations, they, as well as the original Deutsch equation, provide only a general approximation for the behaviour of a real precipitator. The most unjustified approximations of the collection efficiency theory which do not hold in the ESPs are as follows.

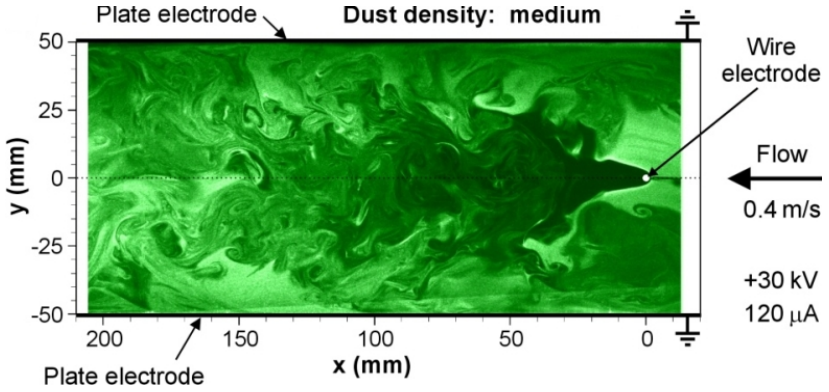

Figure 1. Instantaneous image of the particle flow in the ESP (primary flow velocity: 0.4 m s^{-1}, applied voltage: +30 kV, total discharge current I = 120 μA). The bright places correspond to high density of the dust [54].

It was assumed that the particle concentration across the precipitator cross section is uniform. In reality due to a relatively high charged particle migration velocity brought about by a strong electric field and particle charging near the discharge electrodes, there is a relatively dust-free zone near the discharge electrode, which broadens as the dusty gas moves through the precipitator (figure 1) [54]. Apart from that, the EHD forces produce strong nonuniformity of the particle concentration in the whole volume of precipitator [55-63], forcing the particles to move inside the

electrohydrodynamically-formed flow streams and vortices (figure 2) [64, 65]. This fact has been raised by us in several publications and at conferences [66-69];

It was assumed that all particles once deposited on the collecting walls remain there forever and are not re-entrained (i.e. the capture efficiency is one). In practice, significant re-entrainment does occur (e.g. due to the back-corona discharge which tears-off deposited particles). To include this effect into the theory numerous attempts have been made to improve upon the Deutsch equation. Although these modifications accounts for some of the experimentally observed deviations from the original Deutsch equation, they have no theoretical bases;

In the Deutsch theory only the particle size and its dielectric constant are considered to affect the particle collection. However, practice shows that the particle resistivity is of major importance, causing reduction of the particle collection efficiency at a given voltage and decrease in the maximum voltage attainable without an arc. Both these effects are attributed to an electrical breakdown phenomenon within the dust deposited on a collecting electrode, known as back-ionisation. Back-ionisation is more severe the higher the electrical resistivity of the dust. Several attempts to measure an expected correlation between dust resistivity and precipitator performance have not been conclusive.

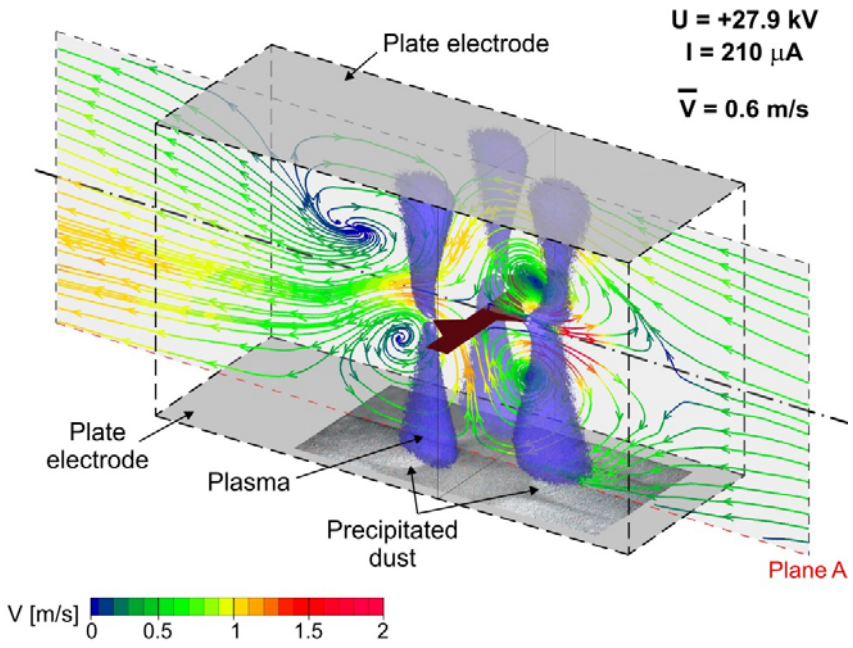

Figure 2. The EHD effects in an ESP with a two-sided spike electrode. Three phenomena are shown: 1) Plasma columns between the spike electrode and collection electrodes (blue–violet colour, 2.5-s photograph exposure), 2) Particle flow streamlines in plane A (coloured continuous lines obtained from PIV measurements, the colour of the streamline in each point corresponds to the magnitude of the velocity vector in this point, see the coloured velocity scale) and 3) Dust deposit on the collecting electrode [65].

Regarding the influence of electrohydrodynamically-induced secondary flow upon the particle collection in a precipitator, the opinions on that are almost equally divided. Some theoretical and experimental papers, rather older, concluded that precipitator efficiency is higher the more laminar the flow, i.e. when the EHD effect is negligible. It means also that precipitators should be more efficient than is predicted by the Deutsch theory, which assumes high turbulence. Those who share this view suggest a careful designing the flow in a precipitator to make it as much laminar as possible. However, the careful design of the laminar flow without taking into account the EHD phenomena cannot be reproduced in a real precipitator, because the EHD forces generate a secondary flow in the discharge

electrode zone, which strongly disturb the primary flow (defined as that far before the discharge electrode zone). The EHD secondary flow is the bulk movement of the neutral gas molecules in the direction of the electric field owing to momentum transfer from the molecular ions. This usually results in a bulk velocity of the gas of (1-2) $m \cdot s^{-1}$ which is comparable with the mean velocity of the primary flow. Better or worse performance of aerodynamically well designed precipitators has not experimentally been identified because too many factors, as, for example, re-entrainment, are important. In recent theoretical and experimental papers, which deal with the EHD secondary flow in precipitators there are suggestions that some flow patterns generated by the EHD forces can improve the performance of precipitators. However, still this dilemma is not unambiguously solved. More fundamental research are needed.

Large precipitators are usually designed with negative high-voltage polarized discharge electrodes because this allows a higher voltage to be applied (without an arc). However, small precipitators, such as those designed for the removal of cigarette smoke in rooms, may have positive high-voltage electrodes, to minimise the production of ozone. The behaviour of EHD flows with negatively or positively polarized electrodes was studied by many researchers mainly in terms of practical aspects relevant to the performance of precipitators (breakdown voltage, ozone production, collection efficiency). The investigations of fundamental processes in the EHD flow for both voltage polarities are still unsatisfactory (e.g. the cause of different EHD flow turbulences for negative and positive voltage polarities and their influence on the particle collection efficiency are unclear).

There is a great need of upgrading the existing precipitators to meet new emission regulations (e.g. the regulation regarding particles of diameter lower than 2.5 μm). There have been several proposals of employing a supplying voltage with a pulsed waveform to improve particle collection efficiency, also fine particles, of the existing precipitators. Such an action was called a pulse energisation. If a short duration pulse is superimposed onto the DC voltage it is possible to obtain a higher peak voltage without sparkover. Owing to it the particle charging improves and the migration velocity increases. Therefore the collection efficiency should increase. In practice voltage pulses of different waveforms have been tested. The improved collection efficiency has been reported only for medium- and high-resistivity particles, which are most difficult to collect. In real precipitators it was found that short pulses give the best improvement in collection efficiency and that there should be a sufficiently long time between pulses to stop sparkover and back-ionisation. Typically there have not been much fundamental research done to understand the EHD effect when the flow is energised by voltage pulses.

Precipitator performance undoubtedly depends upon designs of discharge electrodes. Many designs of electrode have practically been used, including plain straight or twisted wires, and pointed electrodes, having barbed or spike-like geometries. No preference for one design rather than another regarding the collection efficiency has been found. The performance differences between the electrode designs are reduced as the electrode becomes coated with dust particles during operation. An interval-regularity of the discharge along the pointed electrode becomes also the case when a plain wire electrode is coated with dust particles. The cause of that has not thoroughly been investigated. Also the way in which the electrodes of different geometries are coated with particle dust in an EHD flow is not clear, although the dust coated electrodes operate differently from those uncoated. However, in many practical cases the design of the electrode is defined by mechanical considerations rather than by electrical performance.

Another parameter related to the precipitator which influences the EHD flow in ESPs is precipitator geometry. It is obvious that the plate-to-plate spacing and discharge electrode spacing influence the precipitator performance, however, there have only been several rather unjustified suggestions related to the effect of precipitator geometry. The geometry effect is met in small precipitators used, for example, for removing cigarette smoke, as dust filters in air conditioning units, and for collecting carbon soot from diesel engines. In such cases several fundamental studies have to be done to clarify the role of small precipitator dimensions on the EHD flow, the coagulation process of small carbon particles, the charging process of carbon particles having a high electrical conductivity, and eventually the collection of the charged carbon particles.

The analysis of the state of the art in electrohydrodynamics in ESPs suggests a list of subjects which still are of interest when the EHD flows in ESPs are concerned:

a. Properties of the corona and back-corona discharges in EHD flows,
b. Fundamental understanding of the physics of the ionic wind produced by the corona and back-corona discharges in EHD flows,
c. EHD flow structures,
d. Blocking the primary flow by secondary EHD flow,
e. Particles migration velocity in EHD flows,
f. Influence of voltage waveform on EHD flows,
g. Influence of the electrode ESP geometries on EHD flows,
h. Turbulences generation, type of turbulences and how they influence the collection of particles and modify the ionic wind produced by the corona discharges.

Although the above list is long, it does not exhaust the subjects of interest. Further progress in the understanding of EHD flows in ESPs depends on employing newly developed or unique diagnostic methods, such as volumetric gas flow velocity measurement method (simultaneous measurement of the velocity in large volumes, the so called Volumetric Velocimetry (VV) method and the time-resolved flow field velocimetry (2-D or 3-D velocity vector measurement in the plane with high time-resolved PIV). Both methods allow investigating the spatial and temporal behaviour of EHD flows in a unique way, with possible observation of the temporal and spatial evolution of the flows on monitors in real time.

Theoretical and numerical investigations play an essential role in elucidating the EHD flows in ESPs. Recently a considerable progress in this field was made by J. S. Chang's [70, 71] K. Adamiak's [72-74] and other groups [75-77]. Comparison of the experimental results with theoretical and numerical findings is an important tool for a better understanding the EHD phenomena in ESPs.

1.2. The paper objectives

In this paper several selected examples of new experimental results on the EHD flow in ESPs are presented. These selected results concern the EHD flow in:

a) narrow circular and rectangular ESPs with longitudinal wire electrode,
b) narrow transverse and longitudinal ESPs,
c) wide multi-spiked electrode ESPs,
d) self-pumped ESP.

These recent results of experimental studies of EHD effects occurring in ESPs enable further progress in a better understanding of the EHD phenomenon and the coupling of the electric field, electric space charge and the flow in ESPs.

2. Diagnostic techniques for EHD flow studies

At present the most popular EHD flow measuring technique, which had been pioneering introduced by us to study the EHD flow in ESPs [66] is Particle Image Velocimetry (PIV). The PIV technique is described in the next chapter.

Over the last decade for measuring the volumetric flow velocity field standard PIV techniques were used. These include scanning a two-dimensional laser sheet through a volumetric region of the flow (which makes the measurement not instantaneous) or using a "thick laser sheet" (which is not truly a volumetric measurement since the thickness of the sheet is limited to less than 1 cm). These techniques were used in many laboratories, but it appeared unsatisfactory and any further progress in deep study and understanding of the EHD flows was difficult, in particular when temporal behaviour of the EHD flows was concerned.

To measure the instantaneous 3-dimensional and 3-velocity components velocity field within a truly volumetric region, in 2009-2010 a VV measuring systems were developed by Dantec Dynamics Inc. and TSI Fluid Mechanics. In their systems the measurement volume is illuminated by

a cone of laser light. The laser emits two very short duration light pulses, separated by a known and adjustable amount of time, similarly as in the "conventional" PIV. As the flow with tracer particles (seeding) passes through the measurement volume, the laser light is scattered by the tracer particles during each laser pulse. A system of 3 or 4 high-frame-rate cameras captures separate images of the scattered laser light for each of the respective laser pulses within the entire measurement volume. Then using a sophisticated imaging technique, image transfer system and computer algorithms the complete 3-dimensional 3-velocity component velocity field is determined. For flows with a low particle number density, a volumetric particle tracking velocimetry algorithm is used. Flows with medium seeding density require a tomographic particle tracking velocimetry algorithm, and highly seeded ones use the least-squares matching algorithm. Unfortunately, both the VV measuring systems offered by Dantec Dynamics Inc. and TSI Fluid Mechanics and the measuring procedures are complex (e.g. illumination and observation of the volume from several directions is needed, which in many cases is impractical). Besides the cost of apparatus is rather high. As a consequence the VV measuring systems of this type have not become popular.

Very recently, in November 2011 a novel single camera instantaneous Volumetric Velocimetry was introduced by Dantec Dynamics Inc. and Raytrix. The introduction of this newly developed Volumetric Velocimetry (VV) is essential for instantaneous 3-dimensional (regarding space and velocity) large-volume observation of the EHD flows, which usually change fast in time (EHD flows are turbulent), and which are 3-dimensional over a large volume. In this new VV system an array of thousands of micro-lenses placed on a single imaging sensor observes the same volume from many perspectives. The observed volume can be reconstructed slice-by-slice at a high accuracy. The applied processing algorithm takes full advantage of Graphical Processing Unit (GPU) to produce results at near real-time. This results in a huge speed increase in getting the flow parameters compared to traditional tomographic or other volumetric techniques. Due to all these inventions the newly offered measuring setup has become much simpler (a single camera) and easier. A careful and tedious cameras alignment and calibration as well as adjustment of Scheimpflug adapters, typical of the previous PIV-based techniques with several cameras are not needed anymore. Not only complexity of both the measuring setup and method but also the cost is substantially reduced, compared to the above-mentioned traditional methods.

Using VV enables us getting information about the large-volume EHD flow in a near real-time. With almost on-line volumetric velocity information available, 3-D visualising and viewing the flow dynamics becomes possible. This greatly helps understanding the spatial and temporal flow structures.

Apart from the these sophisticated diagnostics methods a simple laser visualisation method cannot be forgot because it also delivers useful information on EHD flow patterns [78].

3. Particle Image Velocimetry (PIV)

Particle Image Velocimetry [79] is used to determine the flow velocity vectors in a selected cross-section of the flow, called the observation plane The observation plane is set in the flow by introducing into it a laser beam in the form of a laser sheet (figure 3). Then two approaches of PIV are possible, two- or three-dimensional. When using two-dimensional PIV method (2-D PIV), the laser sheet is assumed to be infinitely thin, and only a single CCD camera is used for monitoring the observation plane. This enables measuring two components of the velocity vectors in the observation plane. The velocity vector measurement is based on observation of the movement of seeding particles that cross the observation plane. The flow seeding particle movement is determined by monitoring the laser sheet light scattered by the particles. The scattered laser light forms the flow image that is recorded by the CCD camera. From two successive images the velocity vectors of the seeding particles can be found. When the seeding particles follow the gas flow, the gas flow velocity in the observation plane can be determined. In the other case, PIV method delivers the particle velocity field in the gas.

Three-dimensional PIV method (3-D PIV) is based on the fact that a real laser sheet has a definite thickness. As a result, three velocity vector components in the observation plane can be determined

when two CCD cameras observing the same measurement area under different angles are used, as shown in figure 3.

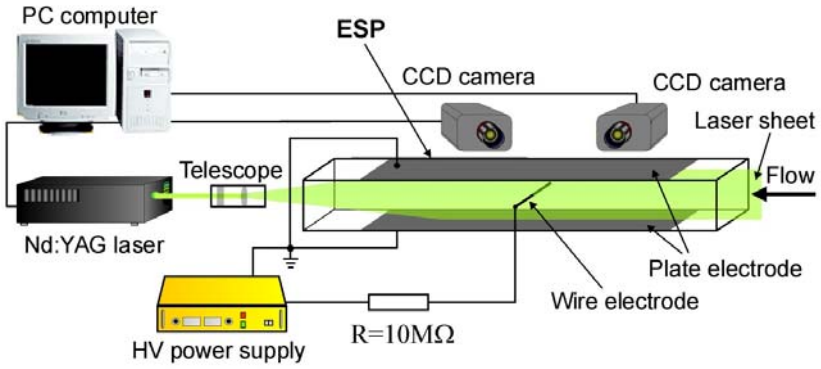

Figure 3. Scheme of set-up for 3-D PIV measurement of flow velocity field in an ESP.

In this paper we present results of new investigations on the EHD flows in ESPs, as mentioned above. In these investigations the PIV equipment consisted of a twin second harmonic Nd-YAG laser system ($\lambda = 532$ nm), imaging optics (cylindrical telescope), one or two CCD cameras and PC computer. The laser sheet of thickness of 1 mm, formed from the Nd-YAG laser beam by the cylindrical telescope was introduced into the ESP to form an observation plane. The images of the particles following the flow in the laser sheet were recorded by two FlowSense M2 cameras. The CCD camera active element size was 1186×1600 pixels. The captured images were transmitted to the PC computer for digital analysis to obtain the velocity map.

The velocity fields presented in this paper resulted from either the instantaneous measurement or the averaging of 100 instantaneous measurements. In the latter case, each velocity map was time-averaged. Based on the measured velocity fields, the flow streamlines were calculated.

4. EHD Flow in Narrow Circular and Rectangular ESPs with Longitudinal Wire Electrode

Recently narrow ESPs have become a subject of interest because of their possible application in diesel engines for the exhausted particulate matter collection [80-82]. Diesel engines emit fine particles, in size range of $7.5 \times 10^{-3} - 1.0$ μm [82], that are harmful for human and animal health. Unfortunately, these submicron particles are not efficiently collected by nowadays ESPs.

The precipitation of particles in the duct of an ESP depends on the dust-particle properties, electric field, space charge, particle physical parameters, electrode geometry and EHD secondary flow. The interaction between the electric field and charge and the flow results in considerable turbulences of the flow which, according to [83, 84], seem to lower the fine particle collection efficiency. They suggested that the flow turbulence should be reduced in order to improve the fine particle collection efficiency. Improving other factors, such as ESP electrode geometry or ESP operating conditions, which influence the flow patterns in ESPs, may also increase the fine particle collection efficiency. In this chapter we present results of 2-dimensional (2-D) PIV measurements of the flow patterns in narrow circular and rectangular ESPs with longitudinal wire-electrode, foreseen for the use in diesel engine exhaust duct to collect fine particles.

4.1. Experimental set-up

The experimental apparatus used in the presented investigation consisted of an ESP, high voltage supply and standard 2-D PIV equipment [85], similar to that shown in figure 3.

The narrow circular ESP consisted of two collecting circular cylinder-electrodes with a longitudinal wire discharge electrode, enveloped by a glass tube (figure 4). The collecting and discharge electrodes were made of stainless steel. Each cylinder-electrode has a length of 100 mm and inner diameter of

25.5 mm. The discharge wire-electrode was 0.23 mm in diameter and 200 mm in length.

The narrow rectangular ESP consisted of four collecting plate-electrodes and a wire discharge electrode, inserted in a glass rectangular cylinder (figure 5). The stainless-steel wire-electrode (diameter of 0.23 mm, length of 100 mm) was mounted in the middle of the ESP, parallel to the main flow direction. The four collecting plate-electrodes (120 mm long and 27 mm wide) were made of aluminium tape of a thickness of 50 μm, glued on dielectric supporting plates.

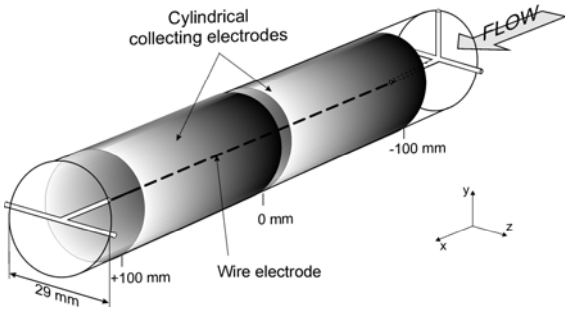

Figure 4. Narrow circular ESP with longitudinal discharge wire-electrode.

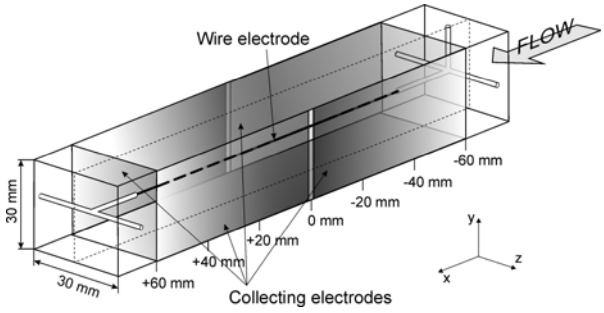

Figure 5. Narrow rectangular ESP with longitudinal discharge wire-electrode.

In both ESPs, positive or negative voltage of 10 kV was supplied to the wire- electrodes through a 10 MΩ resistor. Air flow seeded with cigarette smoke was blown along the ESP duct with an average velocity of about 0.9 $m \cdot s^{-1}$.

The PIV measurements were carried out in the wire electrode mid-plane (i.e. at $x = 0$ mm), perpendicularly to the wire and the collecting electrodes. The velocity fields presented here resulted from the averaging of 100 measurements, which means that each velocity map is time-averaged.

4.2. Results

Instantaneous images of the dust particles and averaged flow patterns (i.e. flow streamlines) in the transverse mid-plane (the y-z plane) of both ESPs are shown in figures 6-7 and 8-9 for circular and rectangular ESPs, respectively.

4.2.1. Circular ESP

The flow patterns in the circular ESP, representing the primary flow motion (i.e. measured without applied voltage not presented here), showed a slight movement of the dust particles in the y-z plane, however, the y- and z- velocity components were very low (below 0.05 $m \cdot s^{-1}$). When a high-voltage was applied to the discharge electrode (figures 6-7), a strong secondary EHD flow was formed in the y-z plane, i.e. transversely to the flow duct. Due to the EHD forces the dust particles moved radially with the migration velocity up to 0.3 $m \cdot s^{-1}$ from the ESP center (i.e. from the discharge wire-electrode) towards the collecting electrodes. The dark circular zones around the wire electrode seen in figures 6a and 7a are the areas from which the particles have already been removed. For the positive voltage polarity, the particle flow towards the collecting electrode was very regular (figure 6b). At the negative polarity, the particle flow pattern (figure 7b) was less regular as for the positive high voltage. The removal of the dust particles from the areas around the wire-electrode may seem faster than in the case of positive polarity (the migration velocity is up to 0.4 $m \cdot s^{-1}$); however, for the negative polarity the discharge current was higher at the same voltage as for the positive polarity.

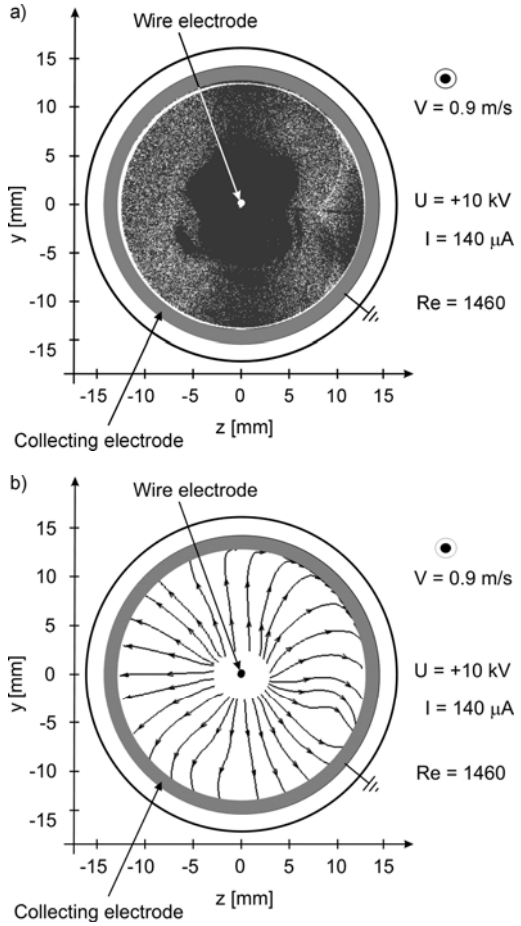

Figure 6. Instantaneous image of the dust particles (a) and averaged flow streamlines (b) in the circular ESP. Average total discharge current 140 μA. Positive voltage 10 kV. ⊙- shows the direction of the primary flow.

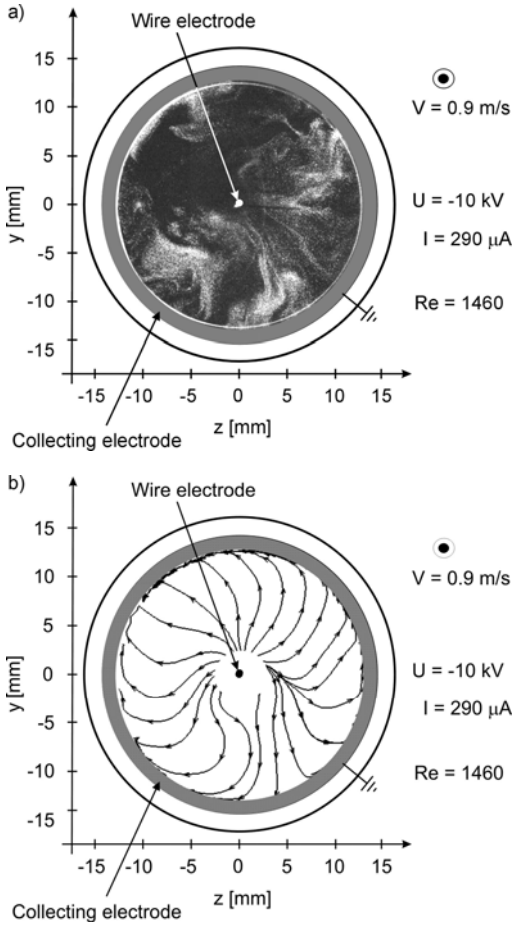

Figure 7. Instantaneous image of the dust particles (a) and averaged flow streamlines (b) in the circular ESP. Average total discharge current 290 μA. Negative voltage 10 kV. ⊙ - shows the direction of the primary flow.

4.2.2. Rectangular ESP

Generally, the particle flow were more disturbed by the applied voltage in the case of rectangular ESP than that in the circular one (figures 8-9). For the positive polarity (figure 8), four streams of the dust particles moved towards the plate electrodes. At the plate electrode, each of the four streams met two oncoming neighboring streams, which results in scattering of the streams. As a result, small twin-vortex structures were formed in all 4 corners of the ESP. The particle migration velocity was up to 0.4 $m \cdot s^{-1}$ f, i.e. slightly higher than in the circular ESP. At the negative polarity (figure 9b) the time–averaged flow pattern confirms the features of the particle flow for positive polarity (figures 8b). Several small vortex structures were formed in the ESP cross section. However, the instantaneous particle flow (figure 9a) was less regular and more turbulent than in the case of positive polarity. The more turbulent character of the flow patterns at negative voltage polarity is probably due to nonuniformity of the negative corona discharge, which exhibits the form of tufts irregularly distributed along the wire in time and space.

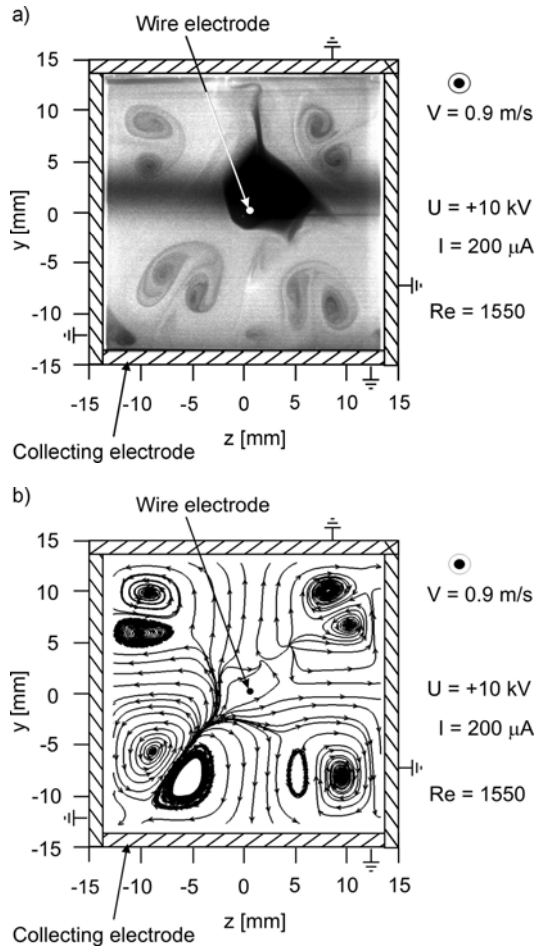

Figure 8. Instantaneous image of the dust particles (a) and averaged flow streamlines (b) in the rectangular ESP. Average total discharge current 200 μA. Positive voltage 10 kV. ⊙ - shows the direction of the primary flow.

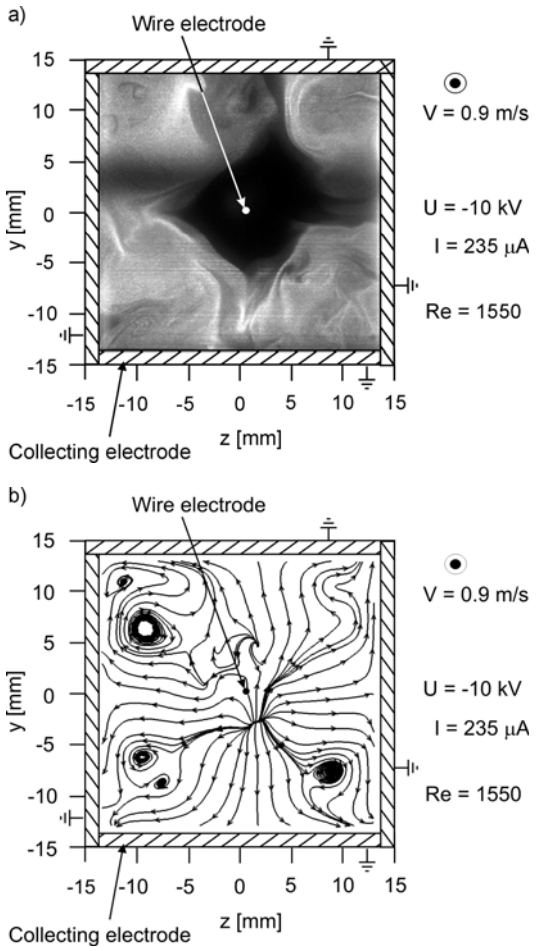

Figure 9. Instantaneous image of the dust particles (a) and averaged flow streamlines (b) in the rectangular ESP. Average total discharge current 235 μA. Negative voltage 10 kV. ⊙ - shows the direction of the primary flow.

4.3. Conclusions

The presented results of 2-D PIV measurements of the particle velocity fields in the narrow ESP showed that the electrode geometry significantly changes the particle flow patterns. Comparing the results for both ESPs (circular and rectangular ESPs) one can see, that flow patterns formed by the EHD forces in the plane perpendicular to the main flow are very different. In the rectangular ESP the particle vortex structures are formed mainly due to the presence of four corners in the rectangular electrode geometry, while in the circular ESP the particles move radially towards the collecting electrodes. It would be interesting to measure the flow patterns in both ESPs along their longitudinal cross-sections. However, it is technically difficult for the circular ESP. The longitudinal flow patterns in the rectangular ESPs measured by us are presented in the next chapter (also in [86]).

The different flow patterns in circular and rectangular ESPs may result in different particle collection efficiency. This subject is under investigation.

5. EHD Flow in Narrow Transverse and Longitudinal ESPs

In this chapter we present investigations of the influence of the EHD secondary flow, generated in a narrow rectangular ESP with transversely or longitudinally to the main flow placed discharge electrode, on the submicron dust particle collection efficiency.

5.1. The ESP

The ESP was an acrylic box (300 mm long, 30 mm wide and 30 mm high) equipped with a wire discharge electrode(s) and two plane collecting electrodes. The experiments were carried out for two discharge wire electrode (diameter of 0.23 mm) positions: transversely- or longitudinally-placed in respect to the main flow direction (figure 10 and 11). The collecting electrodes (60 or 120 mm long and 30 mm wide) were placed along the ESP at its bottom and top.

In both ESPs (transverse and longitudinal), positive or negative voltage up to 18 kV was supplied to the wire- electrodes through a 10 MΩ resistor. Air flow seeded with cigarette smoke was blown along the ESP duct with an average velocity of about 0.5 $m \cdot s^{-1}$. The laser visualization and PIV measurements of the EHD flow were performed in the x-y plane along the ESP duct (i.e. along the longitudinal plane) at $z = 0$ mm in the transverse ESP and at $z = 5$ mm in the longitudinal ESP.

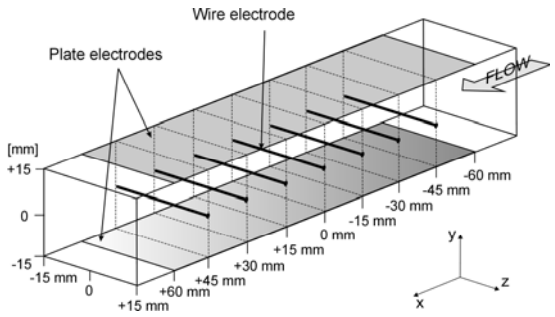

Figure 10. Narrow ESP with transverse wire electrodes.

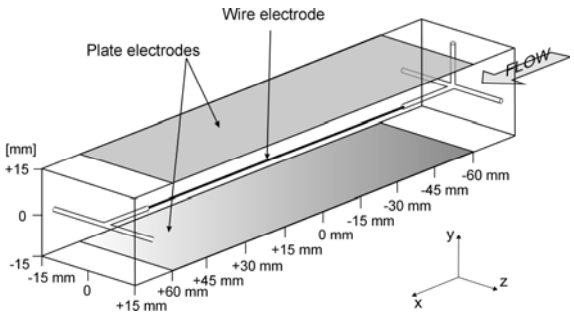

Figure 11. Narrow ESP with longitudinal wire electrode.

5.2. Results

In both narrow ESPs the flow patterns measured without applied voltage (results not presented in this paper) were laminar and the submicron dust particles followed the gas primary flow. After applying a high voltage to the wire electrode/electrodes (figures 12-17), the EHD forces exerted by the electric field on the space charge generated by a corona discharge induced an EHD secondary flow of the gas which altered significantly the primary laminar flow. The seed particles were pushed from the wire electrode(s) outwards by the electric force which was strongest around the wires. The dark areas around the wire electrode/electrodes seen in figures 12-17 are the areas from which the particles have already been removed (the brightness of the image is proportional to the seed particle concentration).

5.2.1. Transverse ESP

In the transverse ESP with one active wire electrode (figure 12), due to the EHD forces the particles moved from the area close to the wire electrode towards the plate electrodes. For the positive voltage polarity the particles flow pattern was regular (figure 12a). The regular dark regions cleared of the dust particles could be easily observed. For the negative voltage polarity the flow structure was rather unstable and turbulent (figure 12b). Moreover, upstream the discharge region near the plate electrodes two vortices were formed (one near the bottom plate electrode and the second one near the top plate electrode).

Increase in the number of the active wire electrodes resulted in a stronger EHD secondary flow (figures 13-15). For the positive voltage polarity the regular structure near the first active wire electrode spread faster towards the collecting electrodes. The flow structures near the subsequent wire electrodes are not so regular and more turbulent. For the negative voltage polarity the flow structures around subsequent wire electrodes are very irregular and turbulent along the channel width. As we show below, the removal of the dust particles in the ESP with negative voltage polarity was faster than in the case of positive polarity.

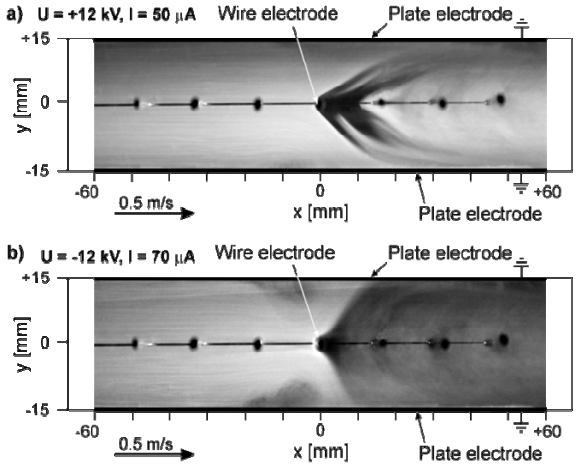

Figure 12. Instantaneous images of the flow structure in the ESP with the one active wire electrode supplied with positive (a) and negative (b) voltage.

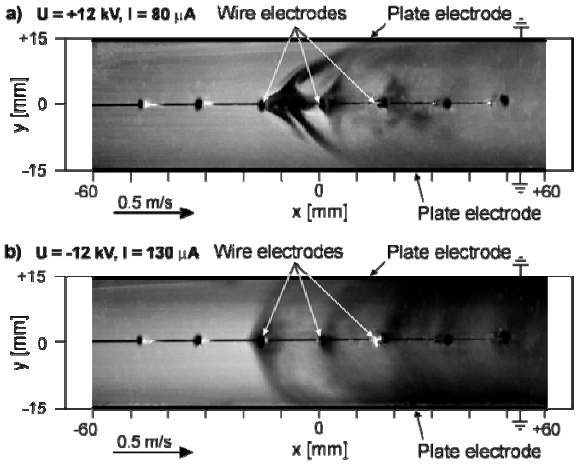

Figure 13. Instantaneous images of the flow structure in the ESP with the three active wire electrodes supplied with positive (a) and negative (b) voltage.

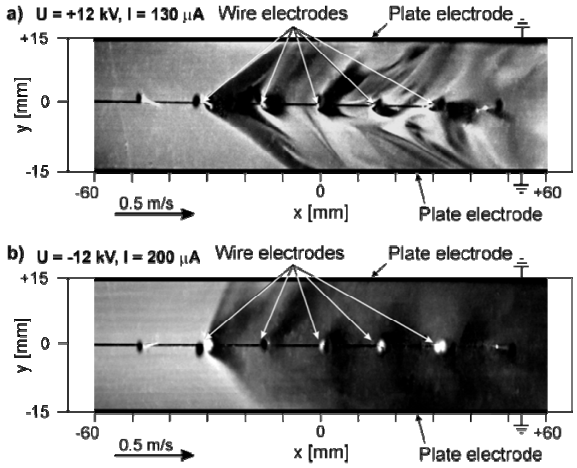

Figure 14. Instantaneous images of the flow structure in the ESP with the five active wire electrode supplied with positive (a) and negative (b) voltage.

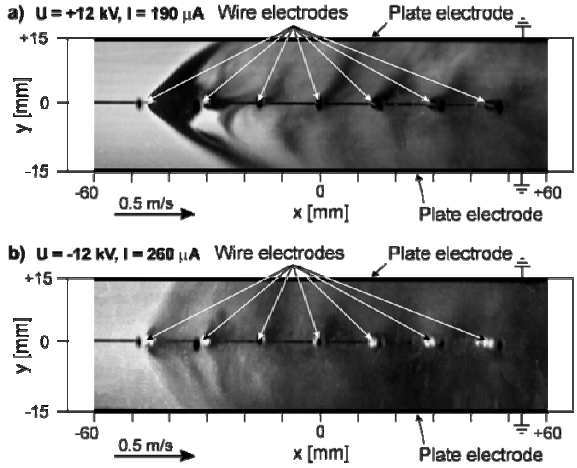

Figure 15. Instantaneous images of the flow structure in the ESP with the seven active wire electrodes supplied with positive (a) and negative (b) voltage.

5.2.2. Longitudinal ESP

Generally, in this case due to the EHD forces the particle flow was formed from the longitudinal wire electrode towards the plate electrodes. The time-averaged flow patterns were very similar for both positive and negative voltage polarities. In both cases, for high voltage of about 9.5 kV, the flow particle trajectories were strongly bent towards the plate electrodes before the discharge region (i.e.at x = -30 mm, figures 16 and 17). However, the most pronounced deflection of the particles towards the plate electrodes occurred between x = -15 mm and x = +15 mm, i.e. in the middle of the discharge region. The particle migration velocity was comparable to the primary flow rate (i.e. V = 0.5 $m \cdot s^{-1}$). For positive polarity a vortex was formed near the upper plate electrode (at around x = -30 mm). Despite similar time-averaged particle flow patterns for both positive and negative polarities, we

observed that the instantaneous particle flow in the longitudinally ESP was less regular and more turbulent in the case of negative polarity, similarly as in the transverse ESP.

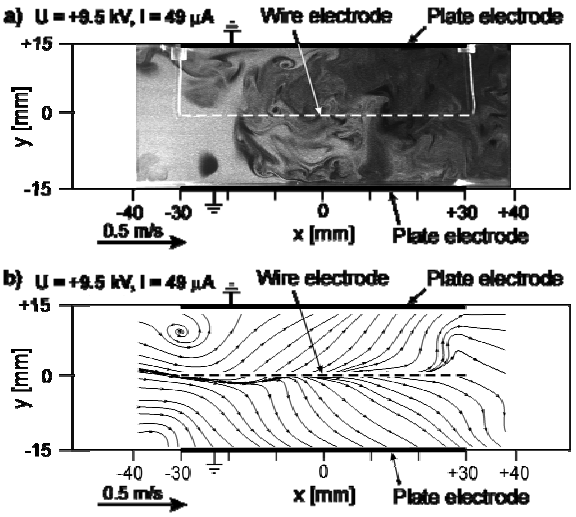

Figure 16. Instantaneous image of the dust particles (a) and averaged flow streamlines (b) in the longitudinal ESP. Average total discharge current 49 μA. Positive voltage 9.5 kV.

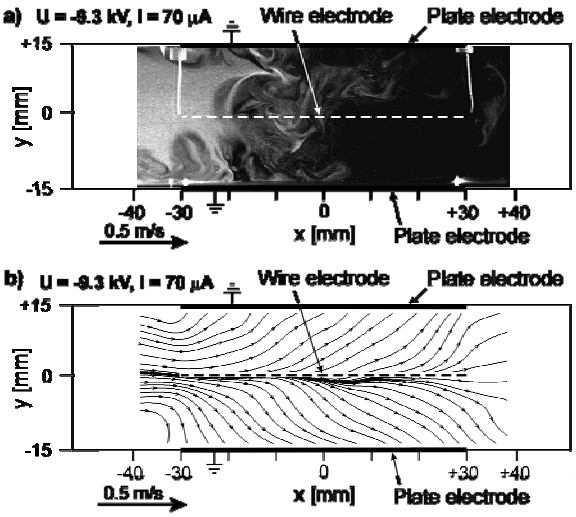

Figure 17. Instantaneous image of the dust particles (a) and averaged flow streamlines (b) in the longitudinal ESP. Average total discharge current 70 μA. Negative voltage 9.3 kV.

Comparison of the collection efficiencies for transverse and longitudinal ESPs for the total discharge current of 140 μA is presented in figure 18. It is seen in figure 18 that the collection efficiency of the transverse ESP with seven active wire electrodes is higher than in the ESP with lower number of the wire electrodes. The higher collection efficiency for arrangement with seven wire electrodes could be explained by the longest active length of ESP (longer discharge region). Comparing the results for the transverse and longitudinal ESPs with the similar active length of the discharge region, the fine-particle collection efficiency was similar for both ESP, transverse and longitudinal.

We found that the fractional collection efficiency in the narrow ESPs is lower for small submicron particles than for larger ones. The particle collection efficiency increases with increasing voltage, and it is higher for negative voltage polarity.

5.3. Conclusions

The experiment showed very complex flow structures in both narrow ESPs, transverse and longitudinal. The EHD secondary flow strongly depended on the applied voltage amplitude and polarity as well as on the arrangement of the discharge electrodes. For the negative voltage polarity the flow structure is more unstable and turbulent. The flow turbulent character at negative voltage polarity is attributed to nonuniformity of the negative corona discharge, which exhibits the form of tufts irregularly in time and space distributed along the discharge wires.

The measurements of the fractional particle collection efficiency confirmed the common view that the particle collection efficiency in the ESP is lower for small submicron particles than for larger ones. The particle collection efficiency increased with increasing voltage, and it was higher for negative voltage polarity. The obtained results showed that the collection efficiency strongly depends on the active length of ESP. It increases with increasing active length of ESP (i.e. with increasing number of wire electrodes in transverse ESP), and is similar for the narrow transverse and longitudinal ESPs of the similar active length.

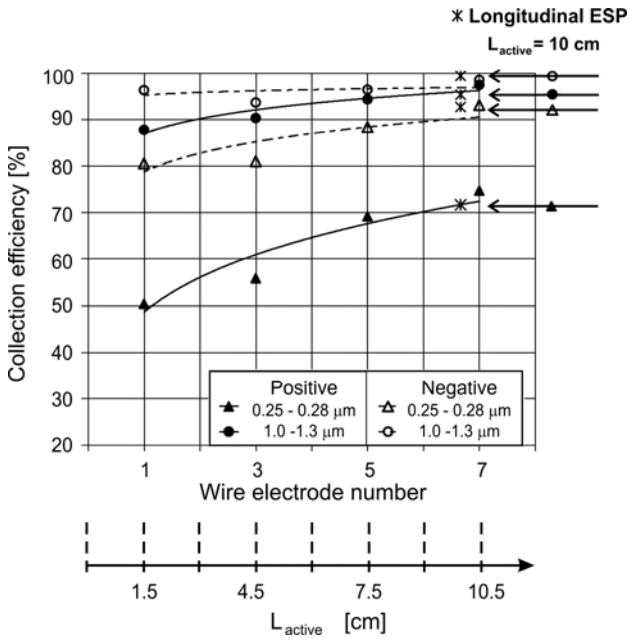

Figure 18. Collection efficiency in the narrow ESPs versus wire electrode number (the total discharge current 140 μA).

6. EHD flow in wide multi-spiked electrode ESPs

In this section investigations of the influence of the EHD secondary flow, generated in an ESP with one-sided and two-sided spike electrodes, on the submicron dust particle collection efficiency are presented.

6.1. The ESP

The duct of the ESP used was made of a transparent acrylic box, 1600 mm long, 200 mm wide and 100 mm high. Such an ESP is classified as a wide ESP. At the top and bottom of the acrylic box two collecting (grounded) stainless-steel plate electrodes (200 mm × 1100 mm) were placed. In the middle of the ESP, between the plate collecting electrodes, a stainless-steel 1 mm thick discharge electrodes were mounted. The distance from the discharge electrodes to the plate electrodes was 50 mm. The distance between neighbouring discharge electrodes was 150 mm. Our experiments were carried out for 2 and 4 discharge electrodes: Two-Sided Spike Electrodes (TSSEs) and a One-Sided Spike Electrodes (OSSEs). The TSSE had 6 spike tips on two sides of the electrode (figure 19a). Two types of the OSSE were used. The first, with 12 spike tips on one electrode side, called an OSSE12 (figure 19b), and the second, with 6 spike tips on one side, called an OSSE6 (figure 19c). In the case of OSSE two electrode arrangements were investigated, i.e. the first, when the spike tips were directed upstream and the second, with the spike tips downstream the primary flow.

The primary flow of air seeded with a cigarette smoke particles was induced by an external fan. The average flow velocity in the ESP duct was controlled using an anemometer. A flow homogenizer was placed before the ESP inlet. During the collection efficiency studies the primary flow average velocity was 0.6 $m \cdot s^{-1}$ ($Re_{0,6} = 3800$). However, at this primary flow velocity the particles were highly collected in the ESP and the PIV measurements were not possible. Thus, the EHD secondary flow measurements were carried out at the primary flow average velocity of 0.9 $m \cdot s^{-1}$ ($Re_{0.9} = 5700$).

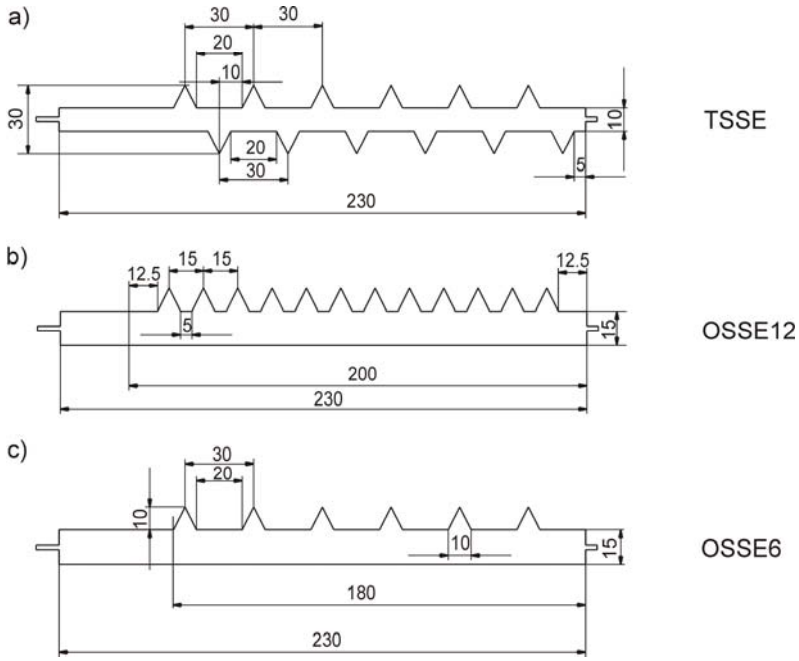

Figure 19. Schemes of the spike discharge electrodes.

The 2-D PIV investigations were carried out in two planes, A and B. In the case of the ESP with TSSEs, plane A passed through the central tip directed upstream; the plane B was passed through the neighbouring tip directed downstream. In the case of the ESP with OSSEs, plane A passed through the central tip; plane B passed in the middle between the central tip and the neighbouring one.

6.2. Results

The EHD secondary flow measurements were carried out for 9 discharge electrode configurations, i.e. with 2 (two) TSSEs, with 2 and 4(four) OSSEs6 directed upstream or downstream, and with 2 and 4 OSSEs12 directed upstream or downstream.

The examples of the flow streamlines in planes A and B obtained for the ESP with 2 TSSEs are presented in figures 20a and 20b, respectively. In this case the negative high voltage of 20 kV was applied and the average total discharge current was 185 μA. As it is seen, in plane A (passing through the spike tip directed upstream) the EHD flow generated near the electrode spike tip (at z = -130 mm and z = 20 mm) blocked the primary flow in the ESP duct centre and directed it to the plate collecting electrodes. However, about 15 mm downstream the spike tip the flow was again redirected towards the ESP duct centre. This was presumably caused by the sucking effect induced by the EHD flow generated near the spike tip directed downstream (figure 20b). We supposed that this effect could be disadvantageous from the particle collection efficiency point of view. Thus, we proposed to use the discharge electrodes with spike tips only on the one side of the electrode (OSSE12 and OSSE6).

In figures 21a and 21b the flow streamlines measured in the ESP with 2 OSSEs12 directed upstream and downstream are presented. The negative high voltage of 20 kV was applied and the average total discharge current was 130 μA (the average total discharge current was independent of the spike tips direction). When the spike tips were directed upstream (figure 21a) the EHD flow generated from the spike tip of the first OSSE12 blocked the primary flow in the ESP centre and directed it to the plate electrodes. The observed flow structure might suggest that many dust particles were collected on the plate electrodes in the area from z = -170 mm to z = -110 mm. The particles not collected in this area flowed along the ESP duct close to the plate electrodes. Then, inflowing in the second OSSE12 discharge region they were relatively far from the discharge electrode and the high

electric field around it. This might be a cause that majority of these particles passed this region without being collected at the plate electrodes.

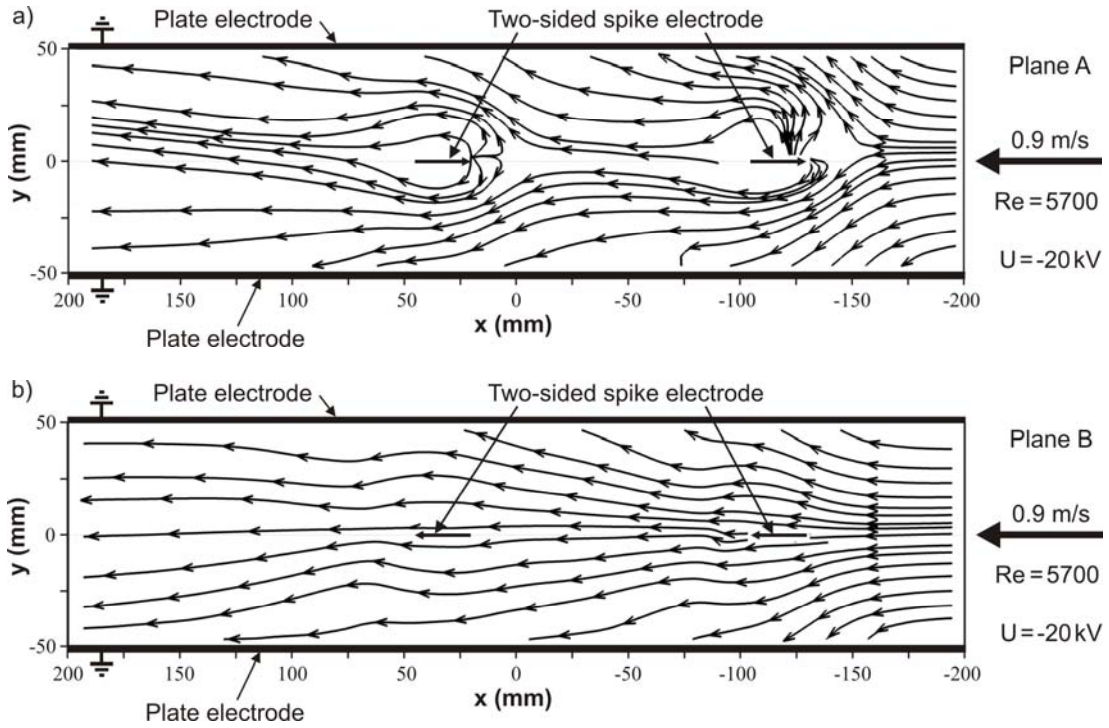

Figure 20. Flow streamlines measured in planes A (a) and B (b) in the ESP with 2 TSSEs. The negative voltage 20 kV, the average total discharge current 185 μA.

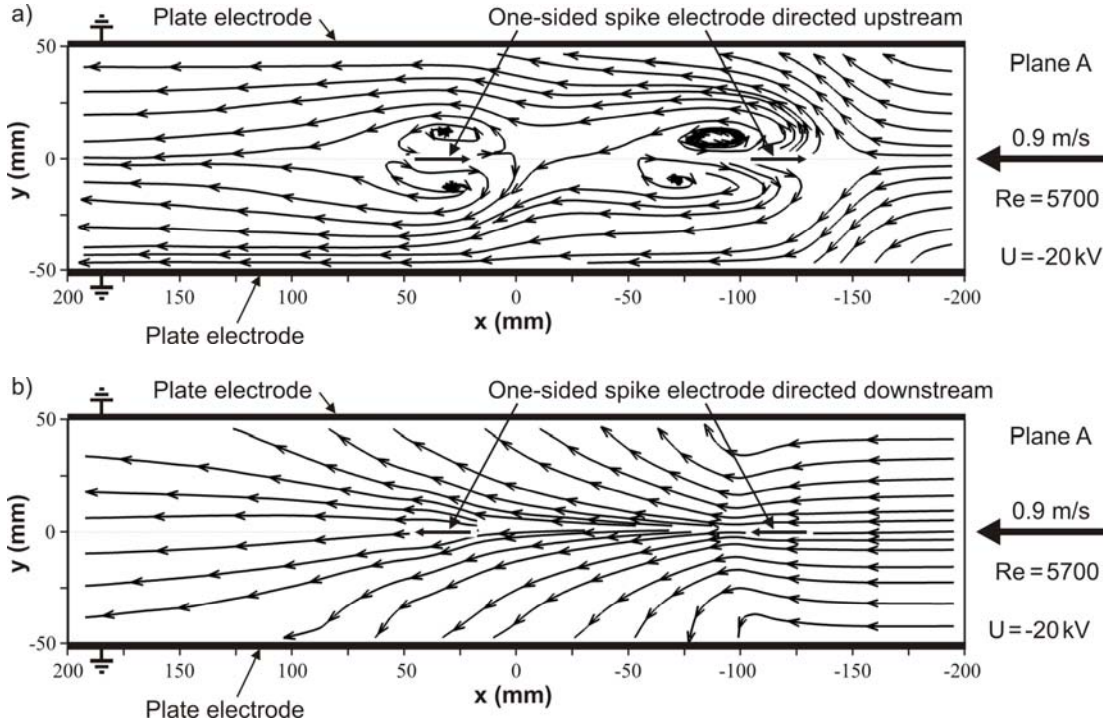

Figure 21. Flow streamlines measured in plane A in the ESP with 2 OSSEs12 directed upstream (a) and dowstream (b). The negative voltage 20 kV, the average total discharge current 130 μA.

The relatively strong EHD flow seen behind the spike tip of the first OSSE12 directed downstream (figure 21b) caused a strong sucking effect. As a result, a flow structure with a very low average velocity near the plate electrodes appeared, and the flow was directed towards the centre of the ESP duct (from z = -130 mm to z = -100 mm). Then, behind the downstream directed spike tip (at z = -105 mm) the dust particles moved through the centre of the ESP duct and quite regularly spread towards the plate electrodes over a large area, eventually reaching the second OSSE12.

The average total discharge current (130 μA) measured when the 2 OSSEs12 were used was much smaller than that of the ESP with the 2 TSSEs (185 μA). Presumably it was due to the short distance between the spike tips of the OSSE12. The discharges generated by each tip interfered with each other which reduced the average discharge current compared to that of the TSSEs. It is known that the lower discharge current results in lower collection efficiency of ESPs. Thus, to avoid this effect we designed another discharge electrode with 6 spikes on one side of the electrode (OSSE6).

Examples of the flow streamlines measured in planes A and B in the ESP with 4 OSSEs6 electrodes directed downstream are presented in figures 22a and 22b, respectively. The applied voltage was – 20 kV and the average total discharge current was 240 μA. The obtained flow streamlines were similar to those obtained for the ESP with OSSEs12. In plane A the flow first moved through the centre of the ESP duct and then scattered towards the plate electrodes. In plane B (in this case placed between the spike tips) only a small flow from the ESP centre to the plate electrodes was observed.

Comparing the flow patterns measured in planes A and B, it can be concluded that for all investigated electrode configurations the EHD secondary flow in the ESP was three-dimensional.

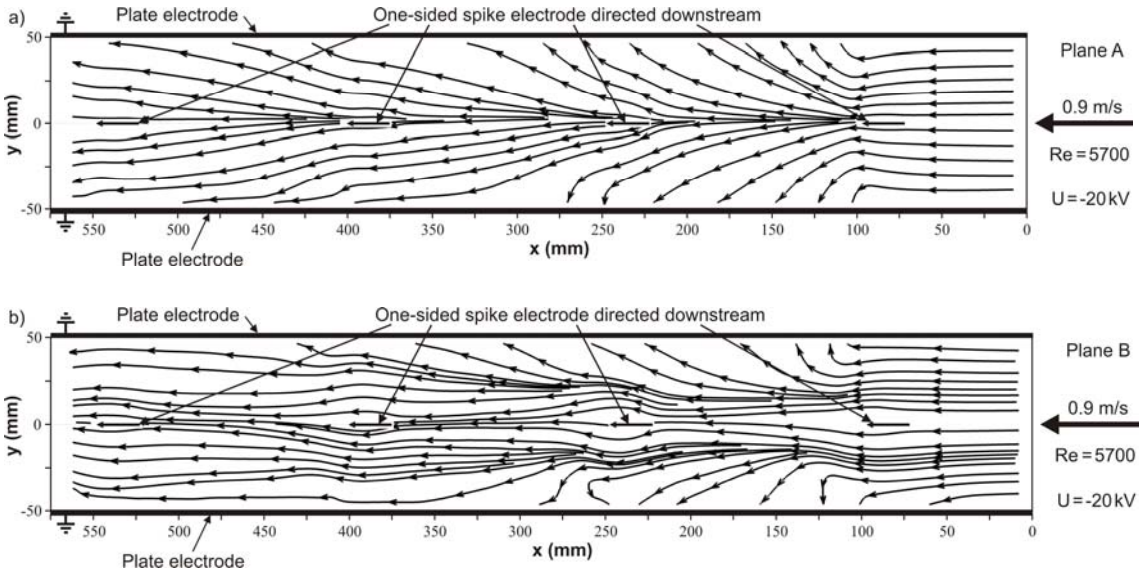

Figure 22. Flow streamlines measured in planes A (a) and B (b) in the ESP with 4 OSSEs6 directed downstream. The negative voltage 20 kV, the average total discharge current 240 μA.

The fractional particle number collection efficiency measurements, in the particle size range from 0.25 μm to 32 μm, were carried out for the ESP with 4 TSSEs, with 2 and 4 OSSEs6 and with 2 and 4 OSSEs12. In the case of OSSEs two electrode arrangements with the spike tips directed either upstream or downstream the primary flow were investigated. Here we present only the results for submicron particles of a diameter from 0.25 μm to 0.28 μm (the average particles diameter 0.265 μm).

The dependence of the submicron particle collection efficiency on the discharge power is shown in figure 23. The results presented in this figure were obtained for the ESP with TSSEs and for the ESP with OSSEs6. For comparison, the collection efficiencies for the ESPs with 1 (single) TSSE and 1 (single) OSSE6 are also presented. These results were obtained in our previous experiment [88].

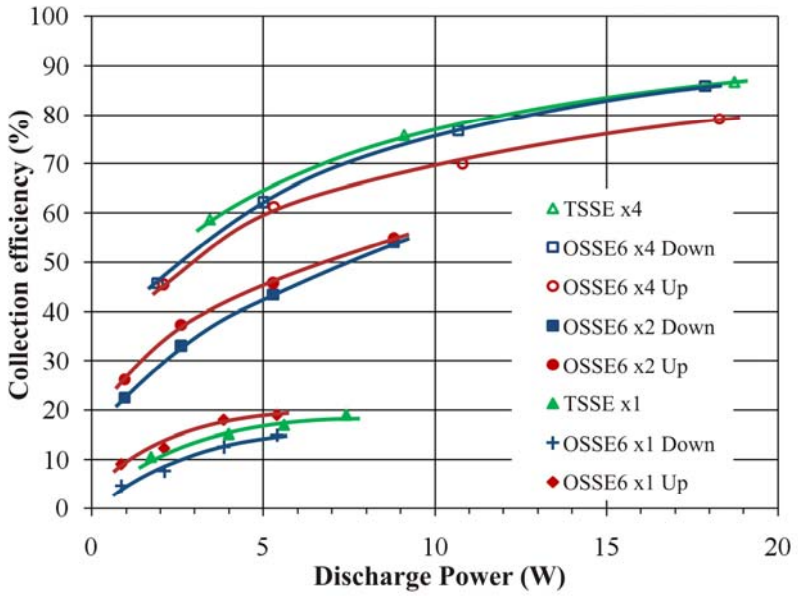

Figure 23. Collection efficiency of submicron particles (a diameter from 0.25 μm to 0.28 μm) in the ESP with TSSEs and OSSEs as a function of discharge power. The negative high voltage. The primary flow average velocity 0.6 $m \cdot s^{-1}$.

As it can be seen in figure 23, in the case of the ESP with a single discharge electrode the highest collection efficiency was obtained when the OSSE6 directed upstream was used. A slightly smaller collection efficiency was obtained when the TSSE was used, and the smallest - in the case of the OSSE6 directed downstream. For the ESP with 2 OSSEs6 higher collection efficiency was again obtained when the spike tips of discharge electrodes were directed upstream (figure 23). However, the difference between collection efficiencies for ESP with 2 OSSEs6 directed upstream and for ESP with 2 OSSEs6 directed downstream was smaller than in the previous case (ESP with a single discharge electrode). The collection efficiencies (figure 23) for the ESP with 4 TSSEs and for the ESP with 4 OSSEs6 directed downstream were almost the same. It is also important to notice that the collection efficiency for the ESP with 4 OSSEs6 directed downstream was higher than for ESP with 4 OSSEs6 directed upstream (unlike the cases of ESPs with 1 OSSE6 and with 2 OSSEs6).

Comparison of the submicron particle collection efficiencies in the ESP with 2 and 4 OSSEs6 and OSSEs12 are presented in figure 24. It can be noticed that a reduction of number of discharge electrode spikes from 12 to 6 almost did not influence the collection efficiency of the ESPs.

6.3. Conclusions

In this chapter the EHD secondary flow and the submicron particles collection efficiency in the spike-plate type ESP with two-sided and one-sided spike electrodes were investigated. The results confirmed that the collection efficiency depends on number, geometry and configuration of the electrodes. The collection efficiency of submicron particles in the ESP with 1 and 2 OSSEs was higher when the spike tips were directed upstream the primary flow. However, when 4 OSSEs were used higher collection efficiency was obtained when the spike tips were directed downstream. Since the ESP working parameters were the same, the obtained results suggest that submicron dust particle collection efficiency in the investigated ESP depended on the induced EHD secondary flow patterns.

From the particle collection efficiency point of view the EHD flow pattern obtained in the ESP with 1 OSSE directed upstream was more beneficial than that formed by 1 OSSE directed downstream. However, in the case of 4 OSSEs directed upstream the EHD flow pattern seemed to hinder the

particle collection, and in consequence the collection efficiency of the ESP with 4 OSSEs directed upstream was clearly lower than that with 4 OSSEs directed downstream.

These examples show how the EHD flow is important when the particle collection in ESPs is considered.

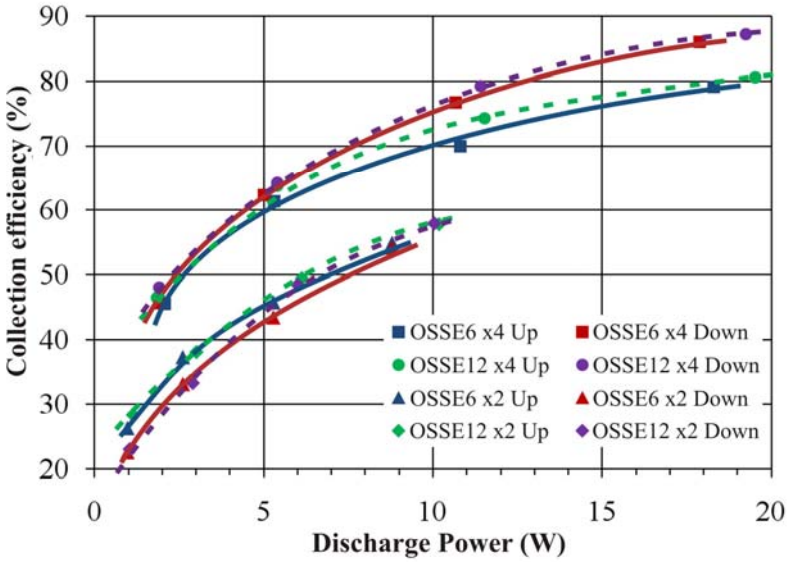

Figure 24. Collection efficiency of submicron particles (a diameter from 0.25 μm to 0.28 μm) in the ESP with OSSEs6 and OSSEs12 as a function of discharge power. The negative high voltage. The primary flow average velocity 0.6 $m \cdot s^{-1}$.

7. EHD flow in self-pumped ESP

In this chapter results of the investigation of EHD flow in a self-pumped ESP e are presented. Our measurements were carried out in an ESP similar to that presented by in [87]. Such an ESP is similar to a typical ESP, however, the gas flow in it is generated by the ESP itself. Therefore, we called this ESP a self-pumped ESP. Such a self-pumped ESP is useful for air cleaning is relatively small rooms, where using a mechanical fan for the ventilation can be bothersome.

7.1. The ESP

The duct of the self-pumped ESP was made of a transparent acrylic box (600 mm long, 150 mm wide and 150 mm high) – figure 25. Inside this box, in the middle of its length, a frame for sustaining spiked high voltage (HV) and grounded electrodes was placed. In the frame two sets of spiked high voltage and grounded electrodes, both made of 1 mm thick aluminium, were mounted. The smooth, grounded electrode and spiked HV electrode were 124 mm wide and 150 mm long. The one of the edges of the HV electrode was ended with 20 spikes. These spikes were 10 mm long. The distance between neighbouring spike tips was 6 mm. The frame sustaining electrodes allowed mounting the HV and the grounded electrodes one above another, thus forming multi-layer electrode arrangement. The distance G between the HV and the grounded electrodes could be changed. The electrodes could also be shifted in the x direction to change the electrode shift X between the edges of the neighbouring electrodes. For the distances G = 15 mm and G = 20 mm the flow patterns near the electrode spikes and the average velocity of the unidirectional flow in the EHD device duct were measured (using 2D PIV method) for the following electrode shift values: X = 8 mm, 15 mm and 50 mm. When the distance G was 20 mm, an electrode set with 3 HV electrodes and 4 grounded electrodes was mounted in the EHD device. In the case of G = 15 mm, an electrode set of 4 HV electrodes and 5 grounded electrodes was formed.

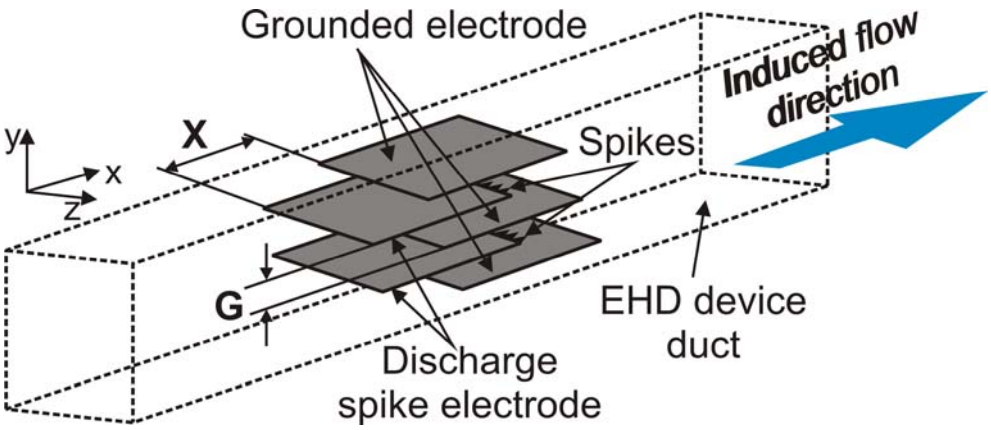

Figure 25. Scheme of the self-pumped ESP for the air cleaning.

7.2. Results

Basing on the PIV measurements, the flow patterns near the spikes of HV electrodes and the average flow velocity induced in the self-pumped ESP duct were determined.

Examples of the obtained flow patterns (streamlines) near HV electrode spikes are presented in figures 26 and 27. The applied DC voltage was 15 kV (positive polarity for G = 15 mm, figure 26; negative for G = 20 mm, figure 27). As it is seen in these figures, a relatively strong EHD flow produced behind the spikes induced significant vortices between the high voltage and the grounded electrodes. For X = 8 mm, the vortices seem to fill almost the whole space between the HV and the grounded electrodes. For X = 15 mm the vortices are slightly smaller than for X = 8 mm, however, the smallest vortices were observed for X = 50 mm. One may expect that strong vortex structures found in the EHD device are capable of hindering the generation of airflow in the EHD device. To check this supposition the average velocity of the unidirectional flow generated in the EHD device for various electrode arrangements was determined.

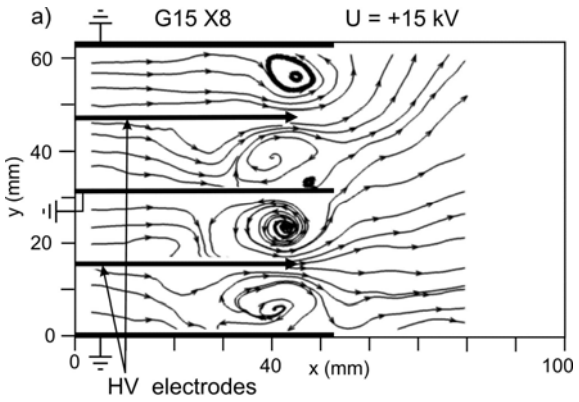

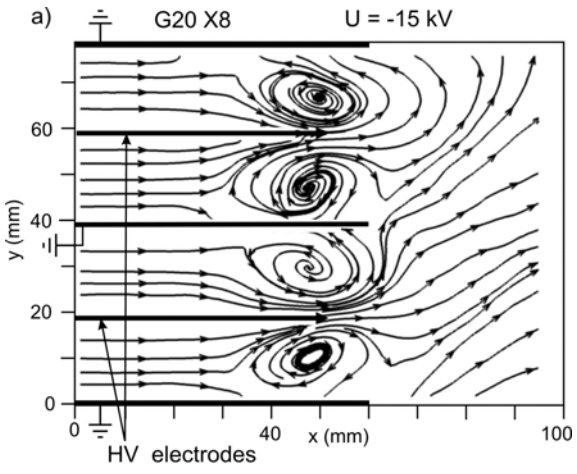

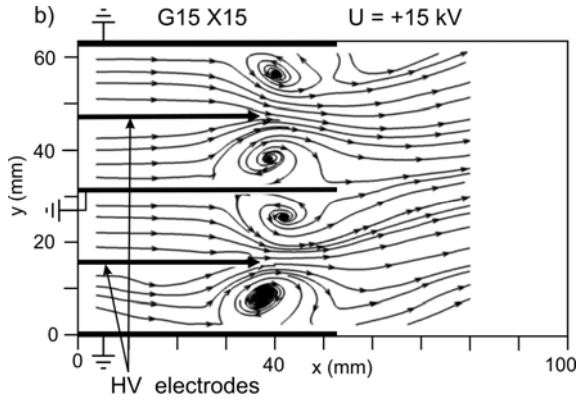

Figure 26. Flow streamlines in the area near the spike tips of the HV electrodes for the electrode arrangements with G = 15 mm, X = 8 mm (a), X = 15 mm (b), X = 50 mm (c). The applied positive high voltage was + 15 kV.

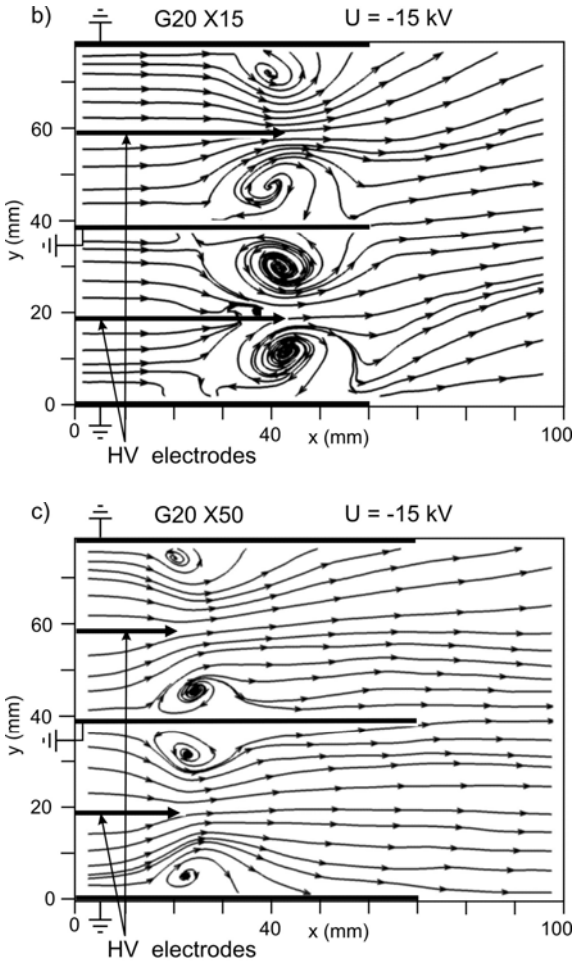

Figure 27. Flow streamlines in the area near the spike tips of the HV electrodes for the electrode arrangements with G = 20 mm, X = 8 mm (a), X = 15 mm (b), X = 50 mm (c). The applied negative high voltage was - 15 kV.

For this purpose, the flow patterns at the EHD device inlet were measured and then the velocity profile was determined at 40 mm before the rear edges of the HV electrodes. Basing on this velocity profile, the average velocity of the induced air flow was calculated. The dependence of the average flow velocity on applied voltage for G = 20 mm and G = 15 mm are shown in figures 28a and 28b. As it can be seen, the average flow velocity increased with increasing applied voltage (with a tendency to saturation). The lowest average flow velocity was found for the X = 8 mm and the highest one for X = 50 mm (as we expected after the streamlines analysis). It seems that in the case of X = 8 mm the majority of applied electrical power was consumed for creating the vortex structures.

The obtained average velocities of the unidirectional air flow (figures 28a and 28b) were slightly higher for negative voltage polarity. The difference in the average flow velocity for the negative and positive polarities was more pronounced for higher voltages. Thus, the electrical efficiency of the unidirectional flow generation the in the EHD device was higher for the negative voltage.

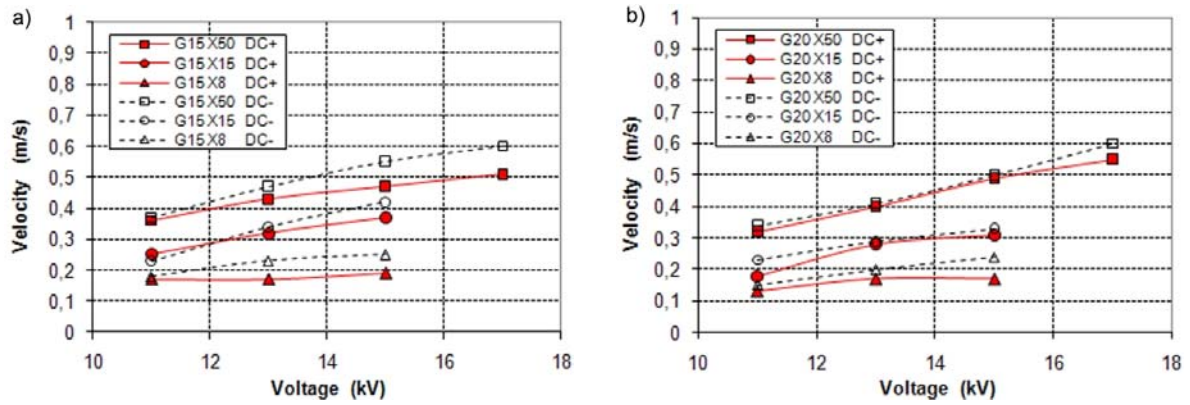

Figure 28. The flow average velocity induced in the self-pumped ESP for (a) G = 15 and (b) G = 20 as a function of the applied voltage

7.3. Conclusions

The results of PIV measurements in the self-pumped spike-electrode ESP showed generation of complex air flow patterns near the spike electrodes and a net unidirectional air flow in the ESP.

The air flow generated by corona discharges behind the spikes induced significant vortices between the spiked electrodes and the grounded electrodes. The diameters of the vortices depended on spiked electrode shift X in relation to the grounded electrode. When the electrode shift X was 8 mm vortices filled the whole space between the HV electrodes and the grounded electrodes. When the electrode shift X was 50 mm, only small vortices near the grounded electrodes were observed. We suggested that the reduction of vortices could be beneficial for inducing strong unidirectional flow in the ESP duct. The results of the measurements of the average flow velocity at the ESP inlet confirmed our suggestions.

The average velocity of the unidirectional flow increased with increasing applied voltage, with a tendency to saturation. The maximum average flow velocity of 0.6 $m \cdot s^{-1}$ was obtained at a voltage of $V_{HV} = -17$ kV for two electrode arrangements, i.e. with G = 15 mm, X = 50 mm, and with G = 20 mm, X = 50 mm.

Our research showed that the presented ESP can also play a role of a fan, thus, the ESP can be useful not only for air cleaning but also for air pumping.

8. Final summary and conclusions

The presented examples of new experimental results on EHD flow in various ESPs showed complex structures of the flow in ESPs, which depend on the ESP geometry, applied voltage and primary gas velocity. The results confirmed an opinion that the EHD flow plays an important role in the particle collection in ESPs. However, despite of delivering many new results, the recent experimental studies did not answer many questions related the influence of the EHD flow on the performance of ESPs. In particular, the influence of the turbulent EHD on submicron particles transport and deposition in ESPs is still ambiguous. This problem and other related to the submicron particle collection in ESPs are to be objectives of further investigations, also theoretical and numerical.

The presented results can be useful in practical implementation, in particular in these industries that use electrostatic precipitators and are subjected to make changes in their technology due to the new air pollution emission regulations.

Acknowledgments

The research presented in this paper was supported by the Ministry of Science and Higher Education grants PB 281/T02/2010/70, PB 327/T02/2010/70, PB 7475/B/T02/2011/40, and by the R. Szewalski Institute of Fluid Flow Machinery, Polish Academy of Sciences, Gdansk

References

[1] Leny R, Leny A M and Boulloud A 1976 *Proc. 4th Int. Conf. Gas Discharges* (Swansea) p 246
[2] Sigmond R S 1976 *Electr. breakdown of gases* (J. Wiley & Sons)
[3] Yabe A, Mori Y and Nijikate K 1978 *J. AIAA* **16** 340
[4] Crichton G C, McAllister I W and Brengsbo E 1979 *Proc. 14th Int. Conf. Phenom. in Ionized Gases* (Grenoble)
[5] Chang J S 1981 *J. Aerosol Sci.* **12** 19
[6] Chang J S, Lawless P A and Yamamoto T 1991 *IEEE Trans. Plasma Sci.* **19** 1152
[7] Chang J S and Watson A 1994 *IEEE Trans. Diel. Electr. Insul.* **1** 871
[8] Peterson R J and Davidson J H 1994 *Proc. IEEE Ind. App. Soc. Ann. Meeting* (Denver) p 1513
[9] Henry R F, Podolski W F and Saxena S C 1985 *IEEE Trans. Ind. Appl.* **21** 939
[10] Dietz P W 1982 *Powder Technol.* **31** 221
[11] Dodbibat G, Shibayama A, Miyazaki T and Fujita T 2001 *Magn. and Electr. Sep.* **11** 63
[12] Jaworek A, Balachandran W, Krupa A, Kulon J and Lackowski M 2006 *Environ. Sci. Technol.* **40** 6197
[13] Carotenuto C, Nataleb F and Lancia A 2010 *Chem. Eng. J.* **165** 35
[14] Hayati I, Bailey A I and Tadros Th F 1986 *Nature* **319** 41
[15] Okuda H 1996 *Phys. Plasmas* **3** 2191
[16] Abu-Ali J and Barringer S A 2005 *J. Electrostat.* **63** 361
[17] Narayanan N, Akkaraju S, Bloomsburgh J and Zhou L *J. Phy.: Conference Series* **34** 704
[18] Kocik M, Podlinski J, Niewulis A, Mizeraczyk J, Tsubone H and Chang J S 2008 *J. Phy.: Conference Series* **142** 012061
[19] Kocik M, Podlinski J, Mizeraczyk J Urashima K and Chang J S 2009 *IEEE Trans. Diel. Electr. Insul.***16** 601
[20] Tanski M, Kocik M and Mizeraczyk J 2011 *IEEE Trans. Diel. Electr. Insul.* **18** 1429
[21] Moreau E 2007 *J. Phys. D: Appl. Phys.* **40** 605
[22] Touchard G 2008 *I. J. PEST* **2** 1
[23] Corke T C, Post M and Orlov D 2009 *Exp. Fluids* **46** 1
[24] Corke T C, Enloe C L and Wilkinson S P 2010 *Annu. Rev.Fluid Mech.* **42** 505
[25] Pons J, Moreau E and Touchard G 2007 *Proc. of 28th ICPIG* (Prague)
[26] Boeuf J P, Lagmich Y, Unfer T, Callegari T and Pitchford L C 2007 *J. Phys. D: Appl. Phys.* **40** 652
[27] Takeuchi N, Yasuoka K and Ishii S 2007 *IEEE Trans. Plasma Sci.* **35** 1704
[28] Balcon N, Benard N and Moreau E 2009 *IEEE Trans. Diel. Electr. Insul.* **16** 463
[29] Takeuchi N and Yasuoka K 2009 *IEEE Trans. Diel. Electr. Insul.* **16** 364
[30] Berendt A, Podliński J and Mizeraczyk J 2010 *Proc. 12th Int. Symp. High Pressure Low Temp. Plasma Chem.* (Trencianske Teplice) p 131
[31] Berendt A, Podliński J and Mizeraczyk J 2011 *Eur. Phys. J. Appl. Phys.* **55** 13804
[32] Forte M, Jolibois J, Moreau E and Touchard G 2006 *Proc. 3rd AIAA Flow Control Conf.* p 2006
[33] Benard N, Balcon N and Moreau E 2008 *J. Phys. D: Appl. Phys.* **41** 042002
[34] Benard N, Balcon N and Moreau 2008 *Proc. 39th Plasmadynamics and Lasers Conf.* p 2008
[35] Benard N, Balcon N and Moreau 2009 *Proc. 47th AIAA Aerosp. Sci. Meeting Incl. New Horizons Forum and Aerosp. Exposition* p 2009
[36] Balcon N, Benard N, Lagmich Y, Boeuf J P, Touchard G and Moreau E 2009 *J. Electrostat.***67** 140
[37] Jolibois J and Moreau E 2009 *IEEE Trans. Diel. Electr. Insul.* **16** 758
[38] Thomas F, Corke T, Iqbal M, Kozlov A and Schatzman D 2009 *AIAA J.* **47** 2169
[39] Benard N and Moreau E 2010 *J. Phys. D: Appl. Phys.* **43** 145201
[40] White H J 1963 *Ind. Electrostat. precipitation* (Addison-Wesley)
[41] Mizuno A 2000 *IEEE Trans. Diel. Electr. Insul.* **7** 615
[42] Jaworek A, Krupa A and Czech T 2007 *J. Electrostat.* **65** 133

[43] Leonard G L, Mitchner M and Self S A 1983 *J. Fluid Mech.* **127** 123
[44] Atten P, McCluskey F M and Lahjomri A C 1987 *IEEE Trans. Ind. Appl.* **23** 705
[45] Chang L and Bai H 1999 *J. Aerosol Sci.* **30** 325
[46] Hoferer B and Schwab A J 2000 *Proc. Conf. Electr. Insul. Diel. Phenom.* p 93
[47] Parasram N T and Taylor A M 2001 *Proc. 8th Int. Conf. Electrostat. Precipitation* (Birmingham)
[48] Blanchard D, Dumitran L M and Atten P 2001 *Proc. 8th Int. Conf. Electrostat. Precipitation* (Birmingham)
[49] Yamamoto T, Okuda M and Ohkubo M 2002 *Proc. Conf. Electr. Insul. Diel. Phenom.* p 228
[50] Fujishima H, Ueda Y, Tomimatsu K and Yamamoto T 2004 *J. Electrostat.* **62** 291
[51] Fujishima H, Morita Y, Okubo M and Yamamoto T 2006 *IEEE Trans. Diel. Electr. Insul.* **13** 160
[52] Adamiak K and Atten P 2009 *IEEE Trans. Diel. Electr. Insul.* **16** 608
[53] Deutsch W 1922 *Ann. Phys.* **68** 335
[54] Podlinski J, Niewulis A, Mizeraczyk J and Atten P 2008 *J. Electrostat.* **66** 246
[55] Yamamoto T and Velkoff H R 1981 *J. Fluid Mech.* **108** 1
[56] Larsen P S and Christensen E M 1986 *Proc. 3rd Int. Symp. Appl. Laser Anemometry Fluid Mech.* (Lisbon)
[57] Self S A, Kihm K D and Mitchner M 1987 *Proc. 3rd Int. Conf. Electrostat. Precipitation* (Padova) p 443
[58] Self S A, Mitchner M and Kihm K D, 1988 *Proc. 7th EPA/EPRI Symp. Part. Contr. Techn.* (Nashville)
[59] Davidson J H and McKinney P J 1989 *Atmosph. Environ.* **23** 2093
[60] Riehle C and Loffler F 1990 *Proc. 4th Int. Conf. Electrostat. Precipitation* (Beijing) p 104
[61] Kanazawa S, Ohkubo T, Nomoto Y and Adachi T 1993 *J. Electrostat.* **29** 193
[62] Hautanen J, Kilpelainen M, Kauppinen E I, Jokiniemi J and Lehtinen K 1995 *Aerosol Sci. Techn.* **22** 181
[63] Soldati A 2000 *J. Aerosol Sci.* **31** 293
[64] Davidson J H and McKinney P J 1991 *IEEE Trans. Ind. Appl.* **27** 154
[65] Podlinski J and Mizeraczyk J 2011 *IEEE Trans. Plasma Sci.* ***3*****9** 2260
[66] Mizeraczyk J, Kocik M, Dekowski J, Dors M, Podliński J, Ohkubo T, Kanazawa S and Kawasaki T 2001 *J. Electrostatics* **51** 272
[67] Mizeraczyk J, Dekowski J, Podliński J, Dors M, Kocik M, Mikielewicz J, Ohkubo T and Kanazawa S 2002 *IEEE Trans. Plasma Sci., 3rd Triennial Spec. Issue "Images in Plasma Sci."* **30** 164
[68] Mizeraczyk J, Dekowski J, Podliński J, Kocik M, Ohkubo T and Kanazawa S 2003 *J. Visualization* **6** 125
[69] Mizeraczyk J, Kocik M, Dekowski J, Podliński J, Ohkubo T and Kanazawa S 2004 *Inst. Phys. Conf. Ser.***178** 167
[70] Cotton J S, Brocilo D, Chang J S, Shoukri M and Smith-Pollard T 2003 *IEEE Trans. Diel. Electr. Insul.* **10** 37
[71] Chun Y N, Berezin A A, Chang J S and Mizeraczyk J 2007 *IEEE Trans. Diel. Electr. Insul.* **14** 119
[72] Farnoosh N, Adamiak K and Castle G 2010 *J. Electrostat.* **68** 513
[73] Farnoosh N, Adamiak K and Castle G 2011 *J. Electrostat.***69** 419
[74] Zhao L and Adamiak K 2008 *IEEE Trans. Ind. App.* **44** 683
[75] Schmid H J, Stolz S and Buggisch H 2002 *Flow Turbul. Combust.* **68** 63
[76] Chun Y N and Yeom D S 2006 *Korean J. Chem. Eng.* **23** 560
[77] Kim S C and Chun Y N 2009 *Int. J. Environ. Pollut.* **36** 337
[78] Mizeraczyk J, Dekowski J, Podliński J, Kocik M, Ohkubo T and Kanazawa S 2003 *J. Visualization* **6** 125

[79] Raffel M, Willert Ch and Kompenhans J 2007 *Part. Image Velocimetry: A pract. guide* (Springer-Verlag)
[80] Zukeran A, Ikeda Y, Ehara Y, Matsuyama M, Ito T, Takahashi T, Kawakami H and Takamatsu T 1999 *IEEE Trans. Ind. App.* **35** 346
[81] Saiyasitpanich Ph, Keenera T C, Khangb S J and Lua M 2007 *J. Electrostat.* **65** 618
[82] Kittelson D B, Reinersen J and Michalski J 1991 *SAE Pap.* 910329
[83] Atten P, McCluskey F M J and Lahjomri A C 1987 *IEEE Trans. Ind. Appl.* **23** 705
[84] Yamamoto T 1989 *J. Electrostat.* **22** 11
[85] Westerweel J 1997 *Meas. Sci. Tech.* **8** 1379
[86] Niewulis A, Podliński J and Mizeraczyk J 2009 *J. Electrostat.* **67** 123
[87] Katatani A and Mizuno A 2010 *J. Inst. Electrostat. Jpn.* **34** 187
[88] Podlinski J, Niewulis A, Shapoval V and Mizeraczyk J 2011 *IEEE Trans. Dielectr. Electr. Insul.* **18** 1401